RPV Irradiation Simulation Using the Contributon Flux Solution

Mario Matijević, Krešimir Trontl, Dubravko Pevec
University of Zagreb, Faculty of Electrical Engineering and Computing
Unska 3, 10000 Zagreb, Croatia
mario.matijevic@fer.hr, kresimir.trontl@fer.hr, dubravko.pevec@fer.hr

ABSTRACT

An important aspect of PWR lifetime monitoring is supporting radiation shielding analyses which can quantify various in-core and out-core effects induced in reactor materials by varying neutron-gamma fields. A good understanding of such radiation environment during normal and accidental operating conditions is required by plant regulators to ensure proper shielding of equipment and working personnel. The complex design of a typical PWR is posing a deep penetration shielding problem for which elaborate simulation model is needed, not only in geometrical aspects but also in efficient computational algorithms for solving particle transport. This paper presents such hybrid shielding approach of FW-CADIS for characterization of the RPV irradiation using SCALE6.2.4 code package. A fairly detailed Monte Carlo (MC) model of typical reactor internals was developed to capture all important streaming paths of fast neutrons which will backscatter of the biological shield and thus enhance RPV irradiation through the cavity region. Several spatial differencing and angular segmentation options of the discrete ordinates (SN) flux solution were compared in connection to an SN mesh size and were inspected by the VisIt code. To optimize MC neutron transport toward the upper RPV head, a particularly problematic region, a deterministic solution of discrete ordinates (SN) in a forward/adjoint mode was convoluted in the so called contributon flux, which proved to be useful for subsequent SN mesh refinement and variance reduction (VR) parameters preparation. The pseudo-particle flux of contributons is coming from spatial channel theory which can locate spatial regions important for contributing to a shielding response.

Keywords: *SCALE, FW-CADIS, RPV irradiation, contributon flux, shielding*

1 INTRODUCTION

The Monte Carlo (MC) simulation of radiation penetration in shields is nowadays a typical routine in nuclear reactor analyses. The maturity of such MC codes and fast pace of computer hardware development have enabled rapid use of this stochastic method for various tasks in nuclear engineering practice, so it is customary nowadays to perform simulations of fuel assembly (FA) burnup-depletion, reactor eigenvalue criticality and radiation shielding on desktop computers and laptops. However, it is easy to find peculiar models which are hard to simulate, not only on desktop computers but also on larger mainframe computing systems, since the brute force method will not circumvent issues with specific particle transport cases. One of such examples is a deep penetration shielding problem posing an impossible task for particles reaching the detector in an analog MC mode or even when using manual variance reduction (VR) techniques in a tiresome trial-and-error way. To alleviate difficulties a hybrid deterministic-stochastic shielding methodology is frequently used when facing such problems [1]. It uses deterministic or mesh-based solution of Boltzmann equation as a means to automatically produce VR parameters which will accelerate final MC

simulation. However, deterministic transport theory methods, most notably discrete ordinates method SN [2], can exhibit certain numerical instabilities if not used properly or without proper understanding since the mesh size (cell aspect ratio), spatial discretization, angular quadratures and Legendre cross section expansion are numerically interdependent.

The objective of this paper was to determine a fairly uniform fast neutron flux distribution in an RPV of a typical PWR reactor, posing aforementioned deep penetration shielding problem, challenging even for hybrid shielding methods. Regarding the model size and complexity level, utilization of any other VR approach, besides a hybrid one, was not justified. A particularly difficult objective was proved to be transporting neutrons from reactor core axially toward the upper reactor head, since massive flux attenuation is present in that region. The backscattering of neutrons on biological shield proved to be an important mechanism for an RPV irradiation which influences the total neutron-gamma distribution.

Even though FW-CADIS (Forward-Weighted Consistent Adjoint Driven Importance Sampling) methodology from ORNL [3][4] was developed for such shielding calculation purposes, it was proved inefficient for obtaining uniformly small MC uncertainties in upper portions of the PWR reactor model. The same slow MC convergence was present for simulation models with denser SN meshes with higher angular quadratures, so a different computational approach was needed. Since the main objective of this paper was to effectively simulate RPV irradiation, from which various dosimetric responses could be derived, it was important to locate spatial regions (or channels) through which fast neutrons will stream through the cavity region, reflect from biological shield and contribute to RPV irradiation. Those important regions that contribute to the desired response are implying the way to perform local SN mesh refinement for improving VR parameters. To facilitate this approach, the concept of spatial channel theory applied to reactor shielding [5] was successfully used on our PWR model.

This paper is organized as follows. Section 2 gives the description of the MAVRIC hybrid shielding sequence, which is part of SCALE6 code package. Section 3 gives a short overview of the contributon theory, which was implemented and used as a computational strategy to improve neutron transport toward the upper reactor head. The PWR simulation model, including neutron-gamma sources, geometry, calculational parameters and VR parameters of FW-CADIS is presented in Section 4, together with influence of SN spatial differencing option on final MC dose distribution. Section 5 gives MAVRIC dose rates inside the PWR model using FW-CADIS basic solution and contributon-informed solution. Section 6 gives discussion and conclusions while the referenced literature is given at the end of the paper.

2 HYBRID SHIELDING WITH SCALE6.2.4

The SCALE6.2.4 code package [6] is a comprehensive modeling and simulation suite for nuclear safety analysis and design. It was developed for the US NRC for the purpose of the evaluation of nuclear facilities and radioactive package designs. The modular structure is in the form of analytical (control) sequences with their functional modules for performing criticality, shielding, radiation source term, spent fuel depletion/decay, reactor physics, and sensitivity analyses. For the purpose of paper brevity, only focus on MAVRIC hybrid shielding sequence is given.

The MAVRIC hybrid shielding sequence [7] is based on CADIS methodology [1] and its generalization for adjoint source weighting using forward flux is known as FW-CADIS [3][4]. Both methods are based on the concept of the so-called importance function, i.e. solution of the adjoint Boltzmann transport equation [8]. These hybrid shielding methods are used for the calculation of space-energy dependent VR parameters in the form of the weight windows (or importance map) and biased source, which work together in tandem. The VR parameters are automatically transferred to functional module Monaco which is a multigroup fixed-source 3D MC transport code. The integrated SN code Denovo [9] is used for solving forward and adjoint fluxes over orthogonal SN

meshes using Koch-Baker-Alcouffe parallel sweep algorithm and nonstationary Krylov methods to solve within-group equations. The results from even intermediate quality Denovo calculation will provide superior VR parameters compared to user's ability to manually tune the same ones. For shielding calculations on point detectors or small regions, CADIS methodology is preferred, and it is based only on adjoint transport solution. For shielding problems with multiple detectors (point and region) or mesh tally over large portions of phase-space, FW-CADIS is preferred to obtain uniformly small response uncertainties [10]. In case of optimizing MC response over a mesh tally, every cell becomes an adjoint source element with inversely weighted strength from forward flux solution. Such an approach will ensure the uniform particle population for distant and close tally objects relative to source regions [11]. In our PWR simulation model, we are interested in global RPV solution of the steady-state transport equation [2] by means of MC particle transport:

$$H\phi = q \tag{1}$$

where H is the linear transport operator, ϕ is the forward flux and q is the total source. The solution to Eq. (1) is first be approximated with forward Denovo SN run. This solution is then used for forward-weighting of the adjoint source (i.e. RPV region), which is used for adjoint Denovo SN run, solving steady-state, multigroup adjoint transport equation

$$H^{\dagger}\phi^{\dagger} = q^{\dagger} \tag{2}$$

where $H^{\dagger}$ is the linear adjoint transport operator, $\phi^{\dagger}$ is the adjoint flux, and $q^{\dagger}$ is the adjoint source. The adjoint source is users' region of interest where optimized MC results are sought; mathematically it is product of the geometric function $g(\vec{r})$ and the energy spectrum corresponding to the response function, which is often cross section $\sigma_d(E)$ for reaction rate calculation or dose function. The adjoint source weighting [7] is done by the integral product of the response function and forward SN flux solution as:

$$q^{\dagger}(\vec{r},E) = \frac{\sigma_d(E)g(\vec{r})}{\int_E \sigma_d(E)\phi(\vec{r},E)dE} \tag{3}$$

An average weight of the MC particle is a space-energy function $\bar{w}(\vec{r},E)$, controlling the process of particle splitting or rouletting during MC transport over the space-energy dependent importance map (or weight windows). This average weight of MC particle is inversely proportional to SN adjoint flux solution as

$$\bar{w}(\vec{r},E) = \frac{C}{q^{\dagger}(\vec{r},E)} = \frac{\iint q(\vec{r},E)\phi^{\dagger}(\vec{r},E)d\vec{r}dE}{\phi^{\dagger}(\vec{r},E)} \tag{4}$$

with C being the normalization constant. The Eq. (4) ensures consistency between source biasing and transport biasing, in a way that birth weight of particle equals target weight in importance map.

3 SHORT OVERVIEW OF THE CONTRIBUTON THEORY

The concept of spatial channel theory is based on generalized reciprocity relation and is used to locate spatial regions that significantly contribute to the response of interest [5][12]. Such identified locations or "spatial channels" are regions more susceptible to particle streaming and thus require additional shielding. This theory originates from 1970-ties work at ORNL on spatial

coupling or forward-adjoint flux folding of 2D discrete ordinates calculations for shielding optimization. A neutron transport operator L for as steady-state form of the transport equation [8] may be defined as

$$L\psi(\vec{r},\hat{\Omega},E)+Q(\vec{r},\hat{\Omega},E)=0, \tag{5}$$

where

$$L\psi(\vec{r},\hat{\Omega},E)=-\hat{\Omega}\nabla\psi(\vec{r},\hat{\Omega},E)-\sigma\psi+\iint\sigma f(\vec{r};\hat{\Omega}',E'\to\hat{\Omega},E)\psi(\vec{r},\hat{\Omega}',E')d\hat{\Omega}'dE'. \tag{6}$$

The transport operator L is not self-adjoint, since inner products (ψ, $L\phi$) and (ϕ, $L\psi$) of two arbitrary functions ψ and ϕ satisfying the required continuity and boundary conditions are different. However, it is possible to define an adjoint operator $L^{\dagger}$ so that for any angular flux ψ we have

$$\left\langle\psi^{\dagger},L\psi\right\rangle=\left\langle\psi,L^{\dagger}\psi^{\dagger}\right\rangle, \tag{7}$$

where $\psi^{\dagger}$ denotes the adjoint angular flux or in short adjoint function. The function ψ will typically satisfy in radiation shielding free-surface boundary condition i.e. $\psi(\vec{r},\hat{\Omega},E)=0$ for all r on the convex boundary with incoming particle directions. This implies a system geometry with a nonreentrant surface, so leaked particle can never be backscattered. Then the adjoint function will satisfy the boundary condition $\psi^{\dagger}(\vec{r},\hat{\Omega},E)=0$ for all r on the boundary with outgoing particle directions. It is assumed that both ψ and $\psi^{\dagger}$ are continuous functions of phase-space meaning no difficulties with gradient calculation, so the difference Δ-term from Eq. (7) becomes

$$\Delta=\iiint\left[\psi^{\dagger}(\hat{\Omega}\cdot\nabla\psi)+\psi(\hat{\Omega}\cdot\nabla\psi^{\dagger})\right]dVd\hat{\Omega}dE, \tag{8}$$

and is required to be zero by definition of self-adjoint operator $L^{\dagger}$. This can be proved by simple interchange of functions and using Gauss theorem to obtain surface integration on which boundary conditions are imposed [8]:

$$\Delta=\iiint\left[\hat{n}\cdot\hat{\Omega}\psi^{\dagger}(\vec{r},\hat{\Omega},E)\psi(\vec{r},\hat{\Omega},E)\right]dSd\hat{\Omega}dE. \tag{9}$$

It is evident that the $\psi^{\dagger}\psi$ product is always zero on the vacuum boundary conditions so it satisfies Eq. (7) which is a familiar reciprocity theorem used in spatial channel theory. It can be recast in a more common form by introducing a fixed forward source $Q(\vec{r},\hat{\Omega},E)=L\psi(\vec{r},\hat{\Omega},E)$ and fixed adjoint source $Q^{\dagger}(\vec{r},\hat{\Omega},E)=L^{\dagger}\psi^{\dagger}(\vec{r},\hat{\Omega},E)$ as:

$$\left\langle\psi,Q^{\dagger}\right\rangle=\left\langle\psi^{\dagger},Q\right\rangle, \tag{10}$$

with the auxiliary condition on observable or response rate $R=\left\langle\psi,Q^{\dagger}\right\rangle$.

These reciprocity equations are frequently used in shielding calculations and show how response rate functional can be calculated easily based on folding an adjoint flux with a forward source, which becomes useful for trending studies, eliminating repetitive forward calculations for a changing source condition. Also, most of the reactor shielding problems have vacuum boundary conditions meaning that this reciprocity theorem will be useful tool for practical calculations. Continuing with theoretical developments [5][12] one would introduce the function which

represents a special type of particles, so-called contributons, which is defined as a product between forward flux and it's adjoint as (in angle integrated, scalar form):

$$C(\vec{r},E)=\phi(\vec{r},E)\phi^{\dagger}(\vec{r},E)\,. \tag{11}$$

The contributon space-energy distribution thus represents the flow of particles in a phase-space, starting from the source region and exiting only through the detector, with no leakage possible since every contributon by definition produces a desired response. Visually inspecting this distribution over phase-space can provide useful information to users; a higher contibution regions represent locations with more contribution to the detector response. Using the standard FW-CADIS methodology in SCALE6.2.4 code, the users can manually construct a scalar contributon distribution by folding multigroup SN solutions for forward and adjoint flux over the structured Cartesian SN mesh. By careful inspection of such contributon distribution, using additional transformations such as normalization and scaling, the user can pin-point important locations and consequently apply local SN mesh refinement for improving deterministic VR parameters for subsequent, accelerated MC simulation.

4 THE PWR SIMULATION MODEL

4.1 MAVRIC model description

The MAVRIC model of the simplified PWR reactor [13][14] was initially developed with SCALE6.1.3 code package [15], but in the meantime was updated for latest version of SCALE6.2.4. It was modified for a detailed RPV fast neutron irradiation simulation, which is an important factor for estimating operational limits and lifetime extension option. The model represents a standard PWR thermal reactor of 2300 MWth with a core consisting of 157 fuel assemblies (15x15 matrix, pitch 21.504 cm), radially surrounded by baffle plates, core barrel thermal shield, RPV, and biological shield. The industrial carbon steel A533B (density 7.83 g/cm^3) with 97.90 w/o Fe and 0.55 w/o Ni was used for the RPV material. The FAs were homogenized and represented with stacked axial regions. Typical industrial and text-book data were used for dimensions and materials of reactor internals, upper and lower RPV heads, biological shield, etc.

The reactor critical core was uniformly sampled with a "flat" spatial profile and Watt spectrum distribution $p(E)=Ce^{-E/a}\sinh(\sqrt{bE})$ for ^{235}U thermal fission (a = 1.028 MeV, b = 2.249/MeV, C is normalization factor). The total neutron intensity for 2300 MWth was halved giving in turn 8.84e19 n/s (i.e. $8.84\cdot10^{19}$) and 2.53e20 phot/s, in order to simulate neutron spatial gradient toward the core periphery. The significant speedup in source sampling during MC simulation was the main reason not to use mesh-based CAAS source [13] prepared in criticality eigenvalue simulation, since it underestimates neutron flux at the core periphery [13]. The fission photon spectrum was explicitly included with a mean value of 7.04 phot/^{235}U fission and secondary gamma emission during neutron interactions. The built-in neutron and gamma axial profiles of typical PWR were used for biasing neutrons during source sampling process in axial direction [6].

The MAVRIC model of the PWR reactor is shown in Figure 1, representing cylindrical global unit of 2140 cm in height and 828 cm in diameter. The boundary conditions were all vacuum type.

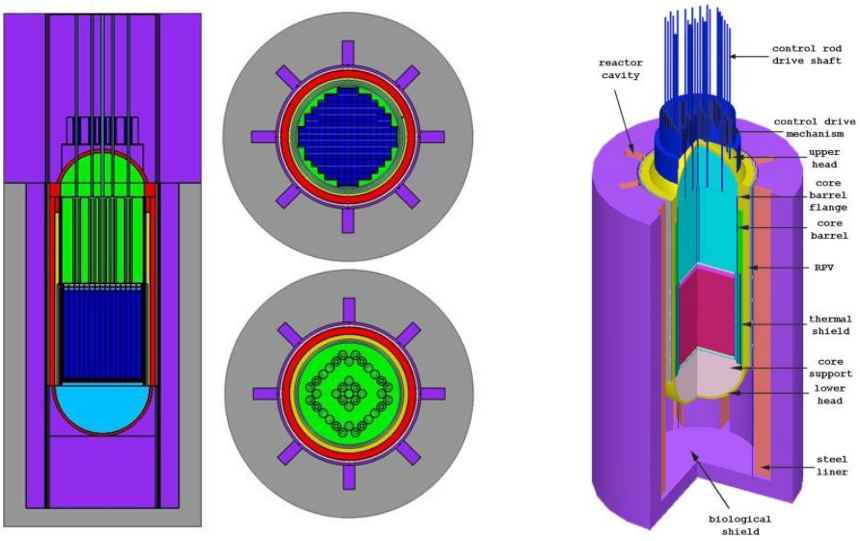

Figure 1: MAVRIC model of the PWR reactor with radial and axial midplanes shown

Several Denovo numerical and control parameters were changed from their default values due to computer memory management. The lower limit of computer memory consumed by the Denovo SN solver in double precision is given as [14]

$$\text{Denovo state size} = N_c (N_g + N_k)(L+1)^2 N_u , \tag{12}$$

where N_c is the number of mesh cells, N_g is the number of energy groups, N_k is the number of Krylov vectors, L is the Legendre order of scattering cross section expansion, and N_u is the number of unknowns per cell by spatial discretization scheme (default is Step Characteristics, SC). The SC differencing has a first-order accuracy [2] i.e., the discretization error decreases linearly with mesh size in the asymptotic limit and requires storage of only one unknown per voxel in memory. It will typically tend to overestimate the fluxes deep within an attenuating material and it always produces positive fluxes for given positive sources. Because of its speed, robustness, positivity, and low memory requirements, it is a default scheme in the MAVRIC code [6]. Since memory consumption grows with $\sim L^2$, we gave preference to a better model voxelization and used S10/P1 for calculations. Accuracy of the SN solution in phase space is not paramount, since even rudimentary solution will accelerate MC convergence. However, the more accurate the importance map is, the fewer histories for MC simulation are needed. The workstation used for this work was quadcore i-5 (3.2 GHz) with 32 GBs of RAM.

4.2 Investigation of spatial differencing scheme

The following results present the influence of spatial differencing on quality of the SN forward-adjoint multigroup solution. The simulation objective was quantification of MC total dose rates in complete RPV region of the PWR model. The option "`AlowShortImpMap`" was used to limit MC transport biasing only to the extent of RPV reduced model. This option will terminate any particles leaving the importance map. As such, MC is not capturing the process of particle back-scattering on biological shield and streaming in cavity region, which will influence the total RPV irradiation with fast neutrons. The RPV was segmented in 6 region tallies, from upper head, ring, radial cylinder to lower head. To capture global MC flux convergence the uniform MC mesh with 2e6 cells (90x90x250) was used.

The Monaco MC was used with 1000 batches with 1e5 neutrons per batch, library was "v7-200n47g" with Centrm xs processing. The Denovo SN was used with "`respWeighting`" option, "v7-27n19g" library, variable spatial differencing, uniform SN mesh with 3.8e6 cells

(110x110x310), S10/P1 parameters with multigroup GMRES solver and tolerance set to 1e-6. Macromaterials were refined with lower value "`mmTolerance`" of 0.0625. The adjoint source was defined using the "`boundingBox`" option and mixture material set to the RPV region with an energy spectrum corresponding to total dose rate function in rem/hr.

To demonstrate the robustness of SC differencing with regard to mesh size and voxel aspect ratios, comparison was done with other higher-level differencing schemes in Denovo[1]. A smooth and continuous adjoint source distribution can be noticed only in SC scheme, which is a key feature for stability of MC transport. In the case of abrupt flux change between neighboring cells one can expect particle oversplitting with abnormally long MC histories leading to “batch freeze” situation. The flux oscillations, zero- and negative-valued flux cells can be mitigated using appropriate weighting, but with increment in CPU time. The comparison of neutron adjoint fluxes and distributed adjoint sources for spatial schemes with one unknown per voxel (SC, DD, DDFF, TWDD) is shown in Table 1.

The linear and trilinear discontinuous schemes have second-order accuracy, but do not ensure positivity. The LDFE and TLDFE methods require storage of four and eight unknowns per voxel, respectively, with similar increase in run time and memory leading to reduced mesh quality for the same allocated RAM. In the case of fine meshes they will give very accurate results but will often break down on coarser grids. The LD scheme tends to be rather sensitive to the aspect ratio of the mesh voxels. While the TLD scheme is more robust than LD, both of them incur a significant memory and CPU time cost, making them generally unfavorable for hybrid shielding.

Table 1: Comparison of adjoint flux (1st row) and adjoint source (2nd row) for different spatial discretization schemes (S10/P1 solution)

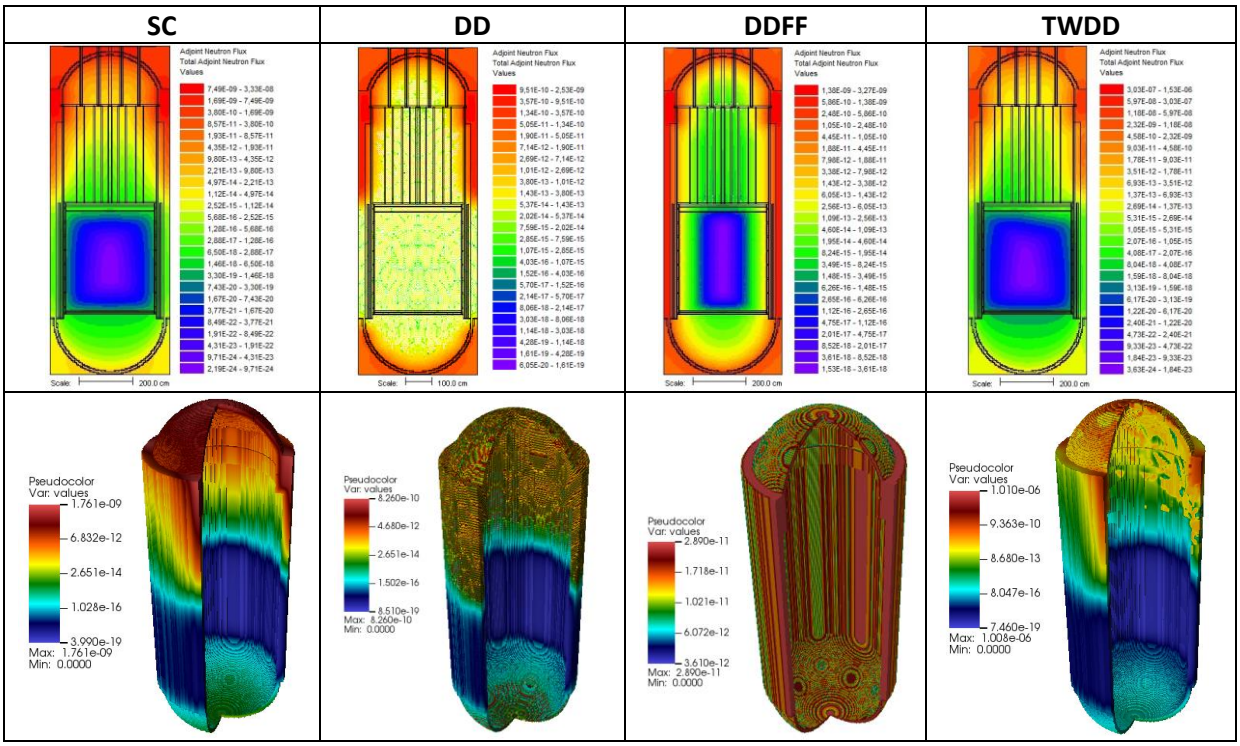

The MAVRIC simulation cases with various spatial schemes using S10/P1 parameters are shown in Table 2 with CPU timing for different FW-CADIS calculation steps. The case-based MC total dose rate distribution is shown in Figure 2, while associated relative errors are shown in Figure 3. It is evident that only SC spatial scheme generated VR parameters which are capable of

[1] DD (diamond difference), DDFF (diamond difference flux-fixup), TWDD (theta-weighted diamond difference), LDFE (linear discontinuous finite element), SC (step characteristic), TLDFE (trilinear discontinuous finite element).

producing uniform flux distribution over the RPV interior. The obtained results also predict the region of upper RPV head and underneath space as the most difficult one for neutron transport, demanding alternative importance map capable of "pushing" neutrons through these highly attenuating materials. This shielding problem was therefore selected for testing contributon-based SN mesh refinement approach but using full MC model and back-scattering of fast neutrons from biological shield in cavity space.

Table 2: The CPU time for different spatial schemes using S10/P1

Spatial scheme	Denovo forward SN (hrs)	Denovo adjoint SN (hrs)	Total Denovo SN (hrs)	Monaco MC (hrs)	Total SN + MC (hrs)
SC	7.69	10.35	18.04	37.04	55.08
DD	4.23	5.81	10.04	6.11	16.15
DDFF	1.30	18.82	20.12	22.58	42.70
TWDD	12.03	16.20	28.23	39.27	67.50
LDFE	6.01	9.09	15.1	89.45	104.55
TLDFE	28.74	39.30	68.04	36.97	105.01

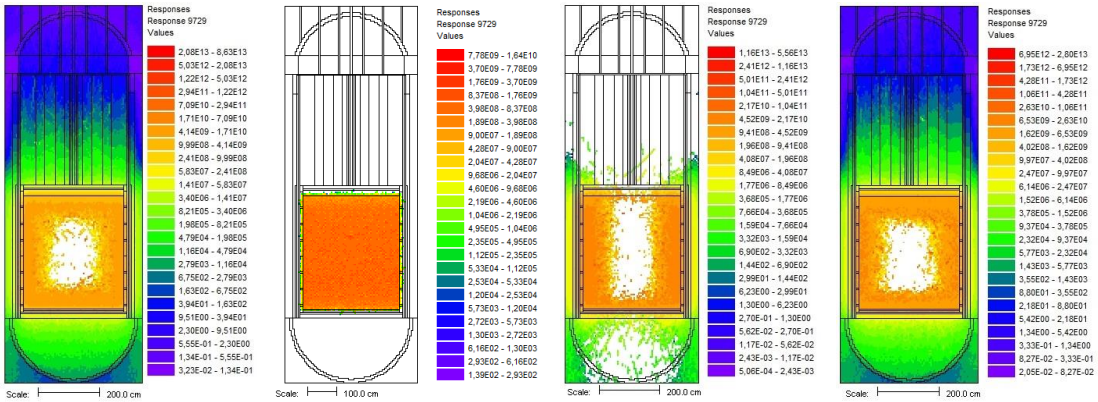

Figure 2: MC total dose distribution (rem/hr) - SC, DD, DDFF, TWDD

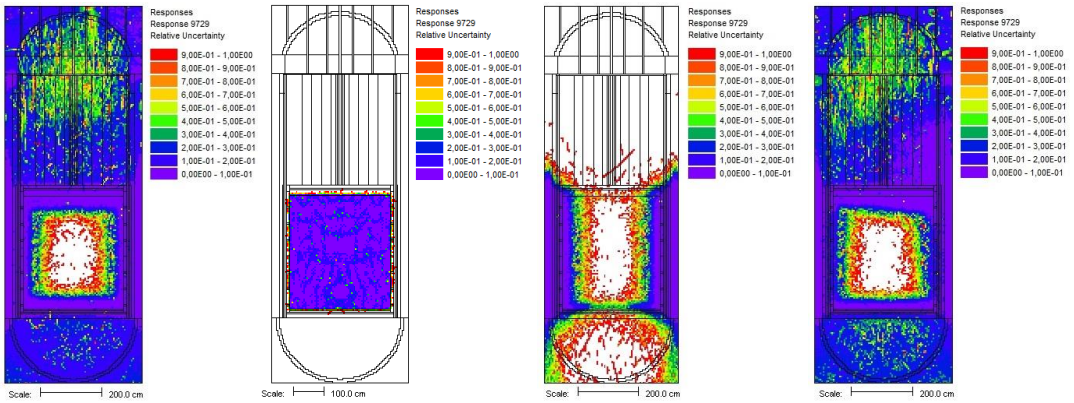

Figure 3: MC total dose relative error - SC, DD, DDFF, TWDD

5 RPV HEAD IRRADIATION USING CONTRIBUTON THEORY

This section demonstrates usage of the contributon theory in the FW-CADIS framework to develop an improved adjoint-forward flux solution by means of local SN mesh refinement. The objective of the calculation is to optimize upper RPV head irradiation by fast neutrons ($E > 0.1$).

Using the total or energy-integrated contributon flux as the information for mesh refinement is a reasonable approach in case of simulating fast neutron transport above 0.1 MeV, i.e. only first 8 energy groups in the broad shielding library "v7_27n19g" and first 106 groups in the fine library "v7_200n47g". Visually inspecting multigroup SN flux solutions in the fast energy range, one can notice a high degree of similarity between group flux profiles, implying overall similar neutron reactions and mean free paths. The energy-integrated flux will thus be a good representative, in an averaged sense, for particle interactions in those fast neutron groups, so user can perform forward-adjoint flux folding to produce a total contributon flux. This approach proved to be useful for fast neutron transport, since only the most energetic neutrons will have the highest probability for reaching the distant RPV regions. In case the user objective is in total flux or dose rates inside RPV, complete neutron spectrum must be taken into account but with gross difference in group-wise flux profiles of forward, adjoint and contributon - this implies how the total contributon flux will not be a good representative for all groups, so group-wise SN mesh refinement would be necessary. For that case, neutron spectrum decomposition is needed, and SN mesh refinement should be done on group-by-group basis using an exact multigroup contributon solution [16].

To summarize our approach: using the total contributon flux for local SN mesh refinement is apparently justified when transporting fast neutrons which is our case of RPV irradiation with neutrons above 0.1 MeV. Auxiliary MAVRIC utilities were used to post-process intermediate Denovo SN results of FW-CADIS methodology in the following steps:

1. Basic FW-CADIS solution of fast neutron flux in RPV head
2. Copy multigroup forward and adjoint fluxes from a temp directory
3. Repair zero or negative cell flux values in forward and adjoint solutions
4. Construct multigroup contributon as product of forward and adjoint components
5. Integrate multigroup contributon to a total or single-group value
6. Normalize total contributon using maximum cell-value
7. Use a high-pass filter to retain contributon values above user defined value[2]

The last point should be commented: the total contributon flux can be "clipped" by manually increasing the lowest distribution value, with an upper value of 1.0 due to normalization. In this way the user has an ability to fine-tune distribution and retain only that amount of information judged to be important for the shielding objective. In this study we have retained the normalized contributon information in three ranges (or cases): a) 1 - 0.1; b) 1 - 0.01; c) 1 - 0.001.

5.1 MAVRIC FW-CADIS basic and contributon-based solution

The basic FW-CADIS solution of RPV head irradiation is presented next. The fast neutron spectrum above 0.1 MeV was prepared in a simple histogram form:

```
response 99
  title="fast neutron spectrum above 0.1 MeV"
  neutronBounds 0.01e-10 1.0e-05  0.1e+06  20.0e+06  end
  values 0.0  0.0  1.0  end
end response
```

The adjoint source was spatially limited to the upper head with a fast neutron spectrum (E > 0.1 MeV). Denovo SN was used with "`respWeighting`" option, S4/P1 with SC spatial differencing, shielding library was "v7-27n19g", lower tolerance of 1e-6 for fluxes, and macromaterial option which produced 450 pseudomaterials from basic 23. The option "`saveExtraMaps`" was activated for keeping intermediate SN results. The SN mesh was uniform with 1.6e6 cells (85x85x220) covering cylindrical global unit (diameter 828 cm, height 2140 cm), giving cell size of cca 10 cm.

[2] Based on engineering judgement by visually inspecting contributon distribution

Monaco MC was used with 10e6 neutron histories (200 batches, 50000 per batch) with "`allowShortImpMap`" option, "`noFissions`" and "`noSecondaries`" options, and fine group shielding library "v7-200n47g". The MC mesh tally was uniform with 2.0e6 cells (92x92x240) covering the same unit, giving cell size of 9 cm. The distribution of forward and adjoint SN source is presented in Figure 4, with a clear effect of source axial biasing and forward-weighting.

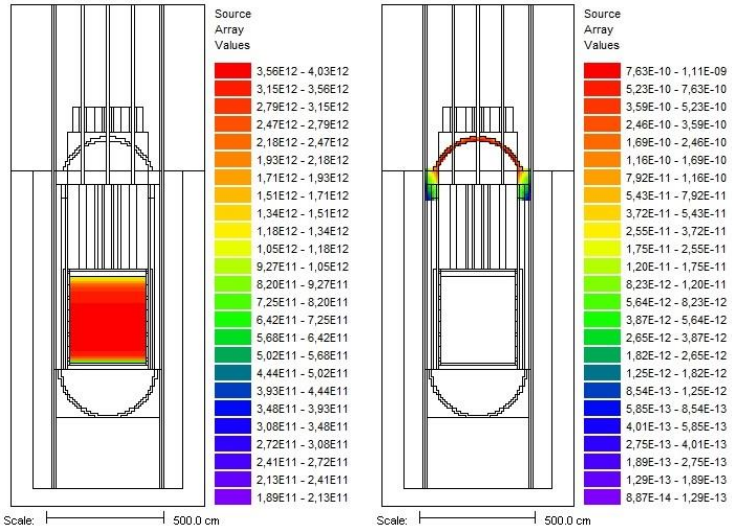

Figure 4: Distribution of forward and adjoint SN source

The distribution of forward, adjoint and contributon flux is presented in Figure 5. It is seen how the axial PWR region above the core has the highest neutron attenuation, effectively shielding the upper head from fast neutrons. The contributon maximum is located in the cavity region of biological shield, indicating intense neutron streaming and back-scattering. Finally, the mesh tally of fast neutron flux with relative errors is shown in Figure 6. The RPV upper head flux was 6.12e4 n/cm^2/s with relative error of 31%, which is statistically not acceptable MC solution after 20 CPU hours. To lower the RPV head error to cca 10%, which would be a satisfactory result regarding the model size, a factor of 9 increase would be needed in histories and CPU time, amounting to 180 hours per run. Even then there is no strict guarantee that MC relative error would decrease as $1/\sqrt{N}$, where N is the number of neutron histories.

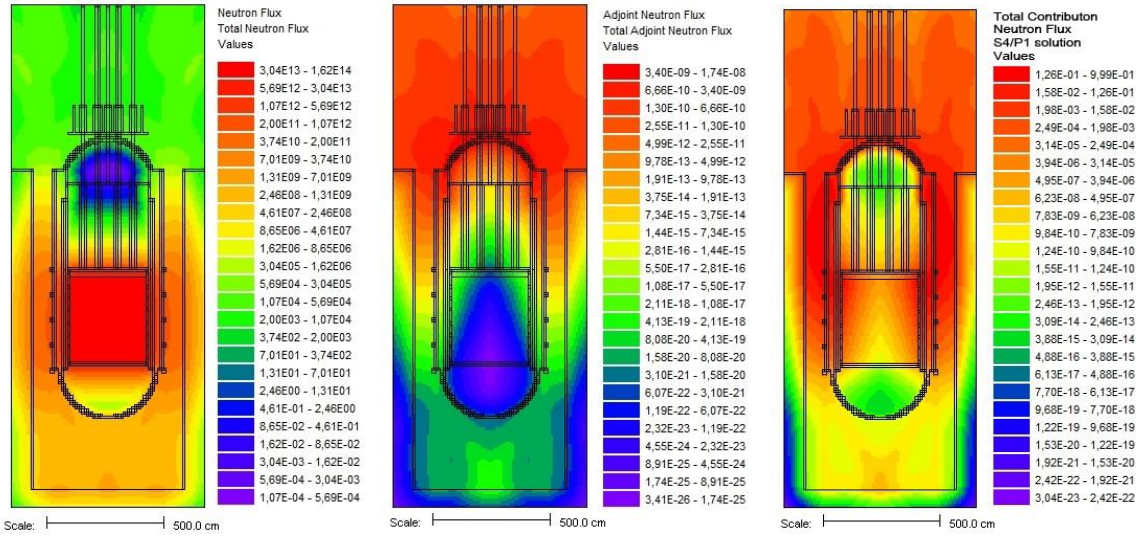

Figure 5: Forward, adjoint and contributon SN flux solution

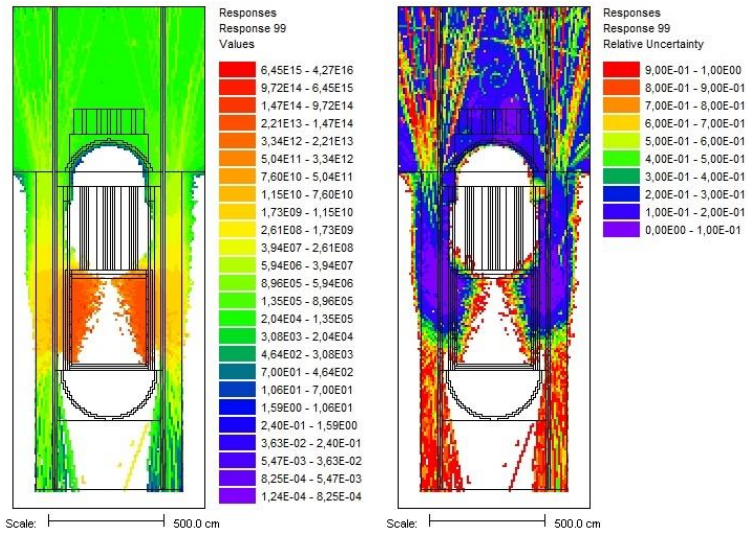

Figure 6: MC fast neutron flux solution (n/cm^2/s) with relative errors

The total contributon flux is now presented in three ranges as stated before and shown in Figure 7: A (1 - 0.1), B (1 - 0.01) and C (1 - 0.001). The fast neutron streaming is very indicative, showing importance of fast neutron scattering on biological shield for upper head irradiation. This phenomenon is pronounced in axial cavity direction (not inside RPV) so SN mesh refinement in z-axis could be an effective method to improve VR parameters. The idea is to locally rebalance SN mesh with a minimum increase in total cell number. For that purpose, a short C-program was written for generating locally refined SN mesh in accordance with contributon ranges, in a format suitable for SCALE input. The mesh refinement process is shown in Figure 8, where smaller cells correspond to important regions by contributon values from Figure 7. It should be emphasized how Denovo works only on Cartesian structured meshes, so every plane defined in *x*, *y* or *z* axis extends through the whole domain.

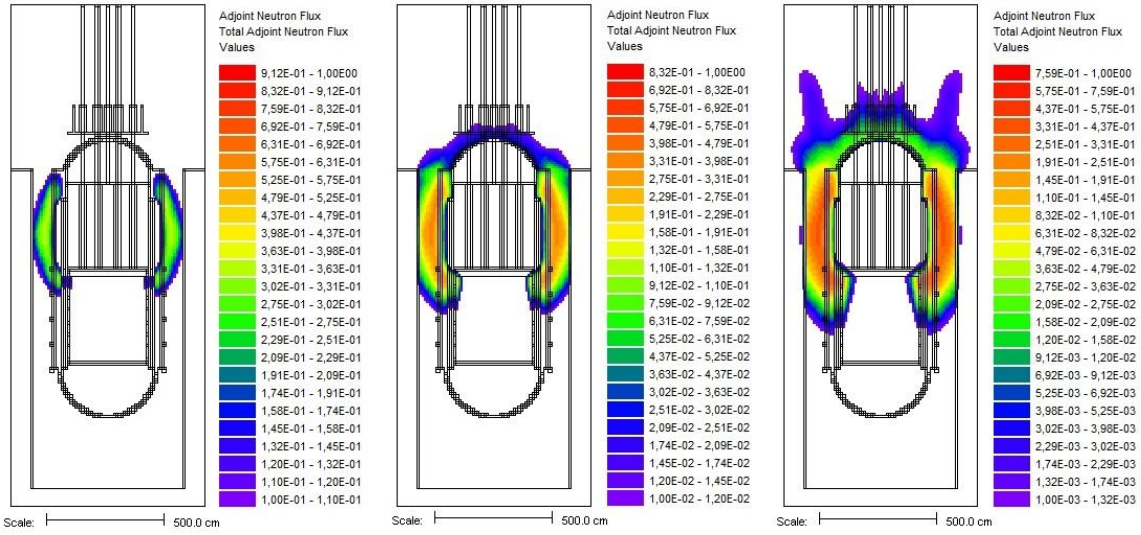

Figure 7: Contributon flux with ranges A, B and C showing important regions

Using such axially refined SN meshes the FW-CADIS shielding calculation of PWR head was repeated three times and the obtained results are presented in Figure 9. A small improvement in overall MC statistics can be seen for range B, but it is more useful to present the obtained results in a tabulated form. Tables 3, 4, and 5 provide such comparison between basic run and contributon runs (A, B, C) with varying order of quadrature sets (S4, S8, S24).

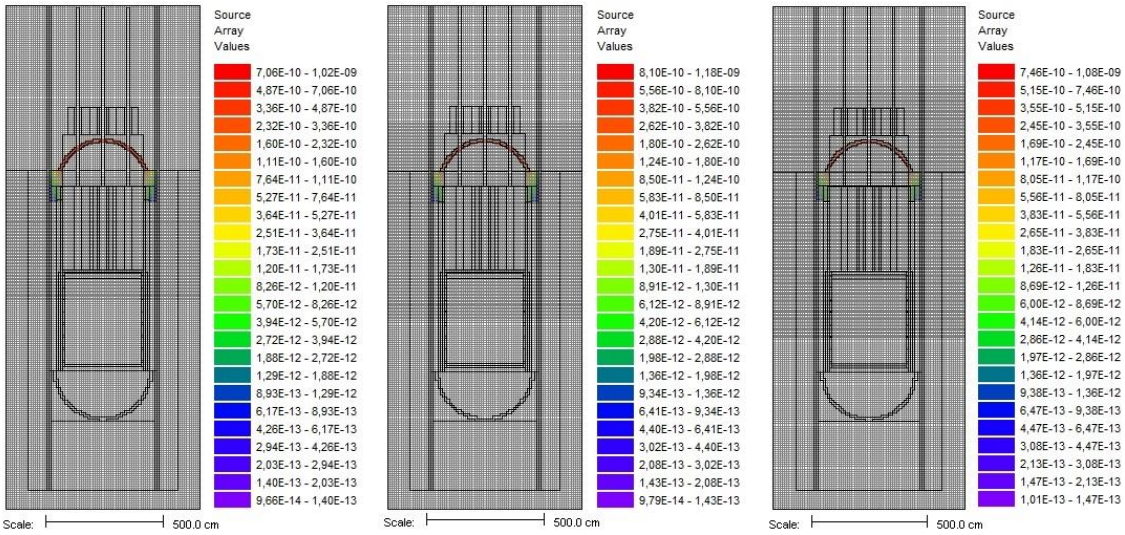

Figure 8: Local SN mesh refinement for contributon ranges A, B and C

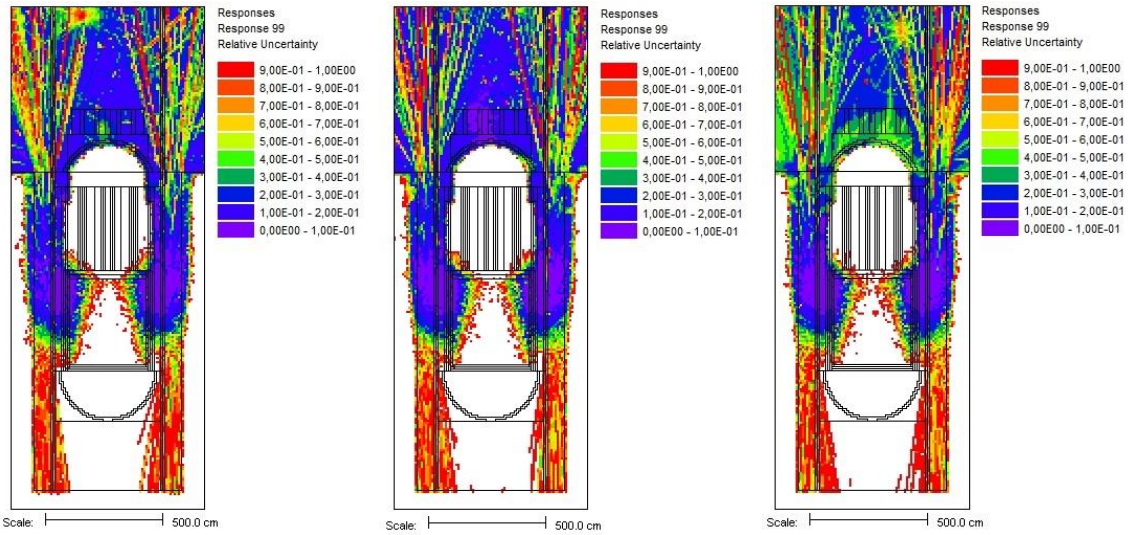

Figure 9: MC fast neutron flux errors for contributon ranges A, B and C

One can notice cases of drastic improvement in upper head MC statistics with a minimal cell number increase for locally refined SN meshes (ratio of SN mesh cells is given in Tables 3, 4 and 5). This is particularly true for S4/P1 variant where refined mesh incurred only 20% more cells but resulted in 3.4 times lower error. The improved quadrature sets resulted in drastic CPU time decrease of MC runs, but only at expense of long SN runs, so total (SN+MC) CPU time gets the same for S4 and S24 sets. Of course, using high-order quadrature sets will produce small values of ordinates μ_N, so to preserve SN flux positivity the mesh spacing should be more stringent in meeting the criterion $\Delta/\lambda < 2|\mu_1|$, where Δ is the cell size, λ is the neutron mfp (mean free path) and $|\mu_1|$ is the minimum value in the quadrature set [2]. Since it's not always easy to meet such criterion with interdependence of SN/PN parameters and mesh size, the proposed step 3. proved to be useful for numerical stability of FW-CADIS. Considering the total CPU time of only 7.9 hrs for reaching similar MC results, it appears how S8/P1 parameters would be suitable for contributon-informed hybrid shielding simulations with FW-CADIS methodology.

Table 3: Influence of contributon range on FW-CADIS with S4/P1

FW-CADIS S4/P1 case	MC upper head flux (n/cm^2/s)	MC error (1 sigma)	FOM (/min)	SN + MC time (hrs)	refined mesh / basic mesh
Basic run	6.12E+04	0.31	8.76E-03	0.8 + 20.0	1.00
Contributon A	6.82E+04	0.26	9.01E-03	0.9 + 26.4	1.18
Contributon B	4.59E+04	0.09	8.62E-02	0.9 + 21.6	1.20
Contributon C	1.27E+05	0.41	3.16E-03	1.0 + 31.2	1.29

Table 4: Influence of contributon range on FW-CADIS with S8/P1

FW-CADIS S8/P1 case	MC upper head flux (n/cm^2/s)	MC error (1 sigma)	FOM (/min)	SN + MC time (hrs)	refined mesh / basic mesh
Basic run	5.90E+04	0.13	1.53E-01	2.2 + 6.8	1.00
Contributon A	4.93E+04	0.09	3.76E-01	2.6 + 5.3	1.20
Contributon B	8.73E+04	0.26	4.04E-02	2.7 + 6.2	1.21
Contributon C	6.24E+04	0.12	1.88E-01	2.6 + 5.8	1.21

Table 5: Influence of contributon range on FW-CADIS with S24/P1

FW-CADIS S24/P1 case	MC upper head flux (n/cm^2/s)	MC error (1 sigma)	FOM (/min)	SN + MC time (hrs)	refined mesh / basic mesh
Basic run	6.84E+04	0.11	4.39E-01	16.2 + 2.9	1.00
Contributon A	5.20E+04	0.08	9.45E-01	17.8 + 2.7	1.09
Contributon B	7.01E+04	0.17	1.98E-01	17.6 + 2.8	1.11
Contributon C	5.70E+04	0.08	9.55E-01	18.2 + 2.8	1.13

Finally, it's worth noting how increasing the axial refinement region by considering contributon flux with a small lower bound, one would lose "locality" of SN mesh refinement and produce a new mesh with a worse aspect ratio of the mesh voxels, i.e. combination of small and large cells. This situation can be seen for S4/P1 variant, case C, where MC error jumped to 41% even though refined mesh had 29% more cells compared to the basic run.

6 CONCLUSION

This paper investigates a potential improvement in FW-CADIS hybrid shielding methodology by using the contributon theory. The contributon flux, created by folding forward-adjoint SN solution, proved to be useful for subsequent local SN mesh refinement and improved variance reduction parameters preparation. The pseudo-particle flux of contributons is coming from spatial channel theory which can locate spatial regions important for contributing to a detector response. This approach was successfully applied to a difficult shielding problem of RPV upper head irradiation by fast neutrons (E > 0.1 MeV). The contributon maximum was noticed in the axial cavity region of the biological shield, implying high influence of neutron streaming and scattering for reaching the RPV upper head. Three ranges of normalized contributon flux were proposed and used for subsequent axial mesh refinement. The refined SN mesh proved to be a rather sensitive to voxel aspect ratio but finally produced improved MC results with minimal increase in cells. Numerical investigation showed how S8 quadrature set on refined mesh produced satisfactory MC result with CPU time decrease of almost 3 times compared to S4 and S24 sets. The obtained conclusions should be however used judiciously, since more numerical investigation is necessary on similar deep penetration shielding problems.

REFERENCES

[1] J.C. Wagner, A. Haghighat, "Automated Variance Reduction of Monte Carlo Shielding Calculations Using the Discrete Ordinates Adjoint Function," *Nuclear Science and Engineering*, Vol. 128, 2, 186, 1998.

[2] E.E. Lewis and W.F. Miller Jr., Computational Methods of Neutron Transport, American Nuclear Society, 1993.

[3] J.C. Wagner, D.E. Peplow, S.W. Mosher, "FW-CADIS method for global and regional variance reduction of Monte Carlo radiation transport calculations," *Nuclear Science and Engineering*, Vol. 176, no. 1, pp. 37–57, 2014.

[4] J.C. Wagner, E.D. Blakeman, D.E. Peplow, "Forward weighted CADIS method for global variance reduction," *Transactions of the American Nuclear Society*, Vol. 97, pp. 630–633, 2007.

[5] M.L. Williams, W.W. Engle, Jr., The Concept of Spatial Channel Theory Applied to Reactor Shielding Analysis, *Nuclear Science and Engineering*, Vol.62, pp. 92-104, 1977.

[6] W.A. Wieselquist, R.A. Lefebvre, M.A. Jessee, Eds., SCALE Code System, ORNL/TM-2005/39, Version 6.2.4, Oak Ridge National Laboratory, Oak Ridge, Tennessee (2020). Available from Radiation Safety Information Computational Center as CCC-834.

[7] D.E. Peplow, "Monte Carlo Shielding Analysis Capabilities with MAVRIC," *Nuclear Technology*, Vol. 174, no. 2, pp. 289–313, 2011.

[8] G.I. Bell, S. Glasstone, Nuclear Reactor Theory, Van Nostrand Reinhold Company, Litton Educational, New York, NY, USA, 1970.

[9] T.M. Evans, A.S. Stafford, R.N. Slaybaugh, K.T. Clarno, "Denovo: a new three-dimensional parallel discrete ordinates code in SCALE," *Nuclear Technology*, Vol. 171, no. 2, pp. 171–200, 2010.

[10] D.E. Peplow, T.M. Evans, J.C. Wagner, "Simultaneous optimization of tallies in difficult shielding problems," *Nuclear Technology*, Vol. 168, no. 3, pp. 785–792, 2009.

[11] J.C. Wagner, D.E. Peplow, S.W. Mosher, T.M. Evans, "Review of hybrid (deterministic/monte carlo) radiation transport methods, codes, and applications at Oak Ridge National Laboratory," *Progress in Nuclear Science and Technology*, Vol. 2, pp. 808–814, 2011.

[12] M.L. Williams, Generalized Contributon Response Theory, *Nuclear Science and Engineering*, Vol. 108, pp. 355-383, 1991.

[13] M. Matijević, D. Pevec, K. Trontl, Dose rates modeling of pressurized water reactor primary loop components with SCALE6.0, *Nuclear Engineering and Design*, Vol. 283, pp. 175-192, 2015.

[14] M. Matijević, D. Pevec, K. Trontl, PWR Containment Shielding Calculations with SCALE6.1 Using Hybrid Deterministic-Stochastic Methodology, *Science and Technology of Nuclear Installations*, Vol. 2016, pp. 1-30, 2016.

[15] "SCALE: A Comprehensive Modeling and Simulation Suite for Nuclear Safety Analysis and Design", ORNL/TM-2005/39, Version 6.1, June 2011. Available from Radiation Safety Information Computational Center at Oak Ridge National Laboratory as CCC-785.

[16] T. Flaspoehler, B. Petrovic, Contributon-Based Mesh-Reduction Methodology for Hybrid Deterministic-Stochastic Particle Transport Simulations Using Block-Structured Grids, *Nuclear Science and Engineering*, Vol. 192, Issue 3, pp. 254-274, 2018.

[17] VisIt: An End-User Tool for Visualizing and Analyzing Very Large Data, VisIt User's Manual, Version 1.5, UCRL-SM-220449, Lawrence Livermore National Laboratory, Weapons and Complex Integration, 2005.